Potential for personal identification using the volume of the mastoid air cells extracted from postmortem computed tomographic images

OURA, Koji
Department of Radiology, Department of Medical Technology, Kyushu University Hospital

IKEDA, Noriaki
Department of Forensic Pathology and Sciences, Graduate School of Medical Sciences, Kyushu University

YOON, Yongsu
Department of Radiological Science, Dongseo University

KATO, Toyoyuki
Department of Radiology, Department of Medical Technology, Kyushu University Hospital

他

出版情報：Legal Medicine. 58, pp.102060-, 2022-09. Elsevier B.V.
バージョン：
権利関係：

Potential for personal identification using the volume of the mastoid air cells extracted from postmortem computed tomographic images

Koji OURA[a], Noriaki IKEDA[b], Yongsu YOON[c], Toyoyuki KATO[a], Junji MORISHITA[e]

[a] Department of Radiology, Department of Medical Technology, Kyushu University Hospital, Fukuoka 812-8582, Japan
[b] Department of Forensic Pathology and Sciences, Graduate School of Medical Sciences, Kyushu University, Fukuoka 812-8582, Japan
[c] Department of Radiological Science, Dongseo University, 47 Jurye-ro, Sasang-gu, Busan, 47011, Korea
[d] Department of Health Sciences, Faculty of Medical Sciences, Kyushu University, Fukuoka 812-8582, Japan

Abstract

This study revealed the usefulness of volumetric analysis of mastoid air cells (MACs) extracted from postmortem CT (PMCT) images for characterizing individuals. To characterize deceased persons, the MAC volumes of 61 Japanese PMCT images were measured after thresholding in Hounsfield units, and based on the number of voxels on the right and left sides and the voxel size for each person. The volume differences between the right and left MACs and the sex were examined. Although there were no obvious volume differences between males and females, the order of sizes on the two sides varied in each person. Moreover, deceased persons could be roughly classified using the total volume of the MACs. Deceased persons who have similar total volumes could be distinguished further by comparing the ratio of volumes in bilateral MACs. Although the identification process is dependent upon samples and different sizes of bilateral MACSs, our pilot study indicated that 81.9% (50/61) of deceased persons could be distinguished. In conclusion, volumetric analysis of MACs measured on PMCT imaging has the potential to identify individuals and reduce the number of candidates.

Key words: personal identification, mastoid air cells, postmortem head CT images, positive identification

1. Introduction

Bones are useful for personal identification and determination of sex, height, and age in forensic anthropology and forensic pathology [1-3]. Ito and Kosuge et al. [4-6] reported radiographic identification for disaster victim identification (DVI). Morishita et al. [7] reported the usefulness of radiographic identification using biological fingerprints to recognize and identify medical images. Advanced imaging techniques, such as high-resolution PMCT imaging, are now available in the fields of forensic anthropology, forensic pathology, and forensic odontology [8-11]. New imaging technologies may provide more accurate and reproducible information than manual measurements, if the conventional identification methods are unavailable or difficult.

Personal identification using paranasal cavities is a conventional method in forensic anthropology and pathology. Studies on the assessment of the paranasal sinus using X-ray imaging have been reported [12]. Virapongse et al. [13] reported the basics of normal pattern and morphology in the pneumatization of the temporal bone in computed tomography (CT) for image interpretation. Isono et al. reported a computer assessment of MACs using CT from the perspective of otolaryngology [14]. However, a detailed and specific methodology for personal identification based on MAC assessment in postmortem CT (PMCT) imaging has not been reported. To examine a new potential for personal identification by using the MACs extracted from PMCT images, this study investigated whether MAC volumes measured on the head PMCT images can be used to identify deceased bodies.

2. Materials and Methods

In total, 61 cases, not including infants, with approval of the institutional review board (40 males, 21 females) were used. All cases were obtained using 16 multidetector raw CT scans (ECLOS, Hitachi Medical Co. (currently FUJIFILM Healthcare Co.), Tokyo, Japan). The matrix and voxel sizes were 512 × 512 mm^2 and 0.978 × 0.978 x 1.00 mm^3, respectively. The deceased bodies was scanned in a cadaver bag before autopsy. Therefore, it was difficult to acquire the same CT positioning as that in antemortem CT imaging (AMCT) in our institution due to postmortem stiffness and decay, in addition to the invisible situation. This situation makes it difficult to measure the reproducibility of the entire volume of MACs and perform further analyses for personal identification.

An algorithm for the measurement of MACs is shown in **Fig. 1**. First, to easily determine the MACs, head PMCT imaging was repositioned similar to that of AMCT imaging, as previously reported [15]. Second, the CT examination table and cadaver bag on the PMCT were removed by threshold processing in Hounsfield unit (HU) values of 40. Subsequently, regions of the MACs on both sides from the top of the temporal bone to the mastoid process were manually contoured at each axial slice of the PMCT, as shown in **Fig. 2**. For the threshold value, -200 HU was employed for distinguishing air and bone components, based on our preliminary study using different MAC sizes (**Fig. 3**). Subsequently, the right, left, and total MAC volumes were automatically calculated based on the number of voxels for the MACs and the product of voxel size.

The total volumes of the MACs were compared for sex-based differences. Statistically significant differences were calculated by Wilcoxon's rank sum test using JMP® (version 12; SAS Institute Inc., Cary, NC, USA). Moreover, manual contouring of MAC regions at each slice was measured 3 times (in September 2018, December 2019, and July 2021) by an operator to check the consistency of the measurement using the interclass correlation coefficient (ICC) within an operator (1,3).

3. Results

The MACs volumes and ratios of large- to small-side MACs are shown in **Table 1**.

The mean MAC volume was 10.97 ± 7.3 mL, not including extremely large cases. The measurement of MAC volumes indicated excellent reproducibility, with an ICC value of 0.993. The volume of the right-side MACs tended to be slightly smaller than that of the left side. Similarly, the volume for females was slightly smaller than that for males (**Table 2).** However, there were no statistically significant differences in either parameter. Moreover, the observed total volume and findings are consistent with those of previous reports [13, 14].

The plots of the total MAC volumes and the results obtained by grouping by every 5 mL are shown in **Fig. 4** and **Table 3**, respectively. These results indicate that narrowing down candidates is possible through rough grouping.

The plots of the right- and left-side MACs, together with the total volume, are shown in **Fig. 5**. The differences in the volumes of both sides varied among individuals. The ratios of the large- to small-side MACs are plotted in **Fig. 6**. If the difference in the ratios exceeded 10%, 81.9% (50/61) cases could be distinguished as different persons, even with similar total MAC volumes.

4. Discussion

In this study, a simple semiautomatic method for measuring the volume of MACS was applied to PMCT images for personal identification. The methods required for personal identification should be speedy and reliable, especially in mass disasters with many victims.

Previous reports using MACs showed no statistically significant difference in classification between the left and right sides and between men and women [13,14,16]. However, we believe that the analysis method based on PMCT imaging still has benefits in understanding more detailed information regarding MACs, and is effective for the future development of personal identification and/or classification methods. According to a previous study [16], mastolytic protrusions were larger in males; thus, it can be assumed that the size or capacity of the masticulary nest is also larger in males. Although MAC volumes depend on race, number of cases, and sex, our mean result (10.97 ± 7.35 mL) falls within the range of previously reported means (2–20 mL; mean, 5.97 mL), with excellent reproducibility [14]. However, more cases should be tested before developing automatic measurements. Moreover, confirmation with the direct determination of MACs [17] may be necessary to establish a reliable identification method.

The reproducibility of the measurements obtained using the proposed method was excellent. The voxel size of the CT scanner was 0.956 mm^3. Therefore, 1 mL corresponds to 1045.5 voxels. If the extracted MAC regions per case had an error of approximately 105 voxels in total, as an example, the volume would have varied by 0.1 mL. To examine the effect of this error, a needle-based volumetric confirmation that uses a syringe and needle to inject water into MACs for measuring the volume of air cells is needed. In addition, the deceased often had fluids in their outer and inner ears. The proposed method was not influenced by the fluids in the ears because the threshold value is suitable for classifying air and other structures, such as water and bone. However, accurate evaluation of the volume is difficult when blood or leachate is present, or when the cause of death involves a region of the MACs.

Rough grouping, as shown in **Fig. 4,** would be useful in narrowing down many candidates, especially mass disasters, such as identifying numerous victims of the Great East Japan Earthquake in 2011 (GEJE 2011) [18]. However, mobile CT scanners and parking spaces for buses are required during these events [8]. Thus, collaboration and preparation of local governments, police, fire departments, hospitals, medical centers, and examiners/coroners should be discussed in detail with forensic pathologists and odontologists before future mass disasters unexpectedly occur. In addition, large-scale databases for DVI must be constructed to realize positive identification.

We found that the deceased had similar total volumes, but different ratios were effective in distinguishing 81.9% (50/61) of the deceased bodies. However, the overall performance changes depending on the

selection of the ratio difference. Greater ratio differences indicate greater reliability in distinguishing the deceased from each other.

Our study indicated the usefulness of PMCT images for personal identification of the deceased. Automatic methods should be developed for a speedier and more effective identification process. However, more cases should be tested before developing automatic measurements. Moreover, confirmation with the direct determination of MACs [17] may be necessary to establish a reliable identification method.

Volumetric analyses of MACs extracted from PMCT images have the potential to narrow down candidates and identify deceased bodies in forensic pathology.

5. Conclusion

Volumetric analyses of the MACs extracted from PMCT images has a potential for narrowing down candidates, and personal identification of the deceased in the field of forensic pathology.

Conflict of interest

We have nothing to declare for this study.

Acknowledgments

The authors thank faculty members of Department of Forensic Pathology and Sciences, Graduate School of Medical Sciences, Kyushu University, Japan, for providing the clinical information for this article.

References

[1] A. Schmitt, E. Cunha, J. Pinheiro, Forensic Anthropology and Medicine: Complementary Sciences from Recovery to Cause of Death, Chapter 14. Humana Press Inc. 2006. ISBN: 978-1-58829-824-9

[2] M. Pfaeffli, P. Vock, R. Dirnhofer, M. Braun, S. Bolliger, M. Thali, Post-mortem radiological CT identification based on classical ante-mortem X-ray examinations. Forensic Sci Int 2007;171: 111-117.

[3] K. Latham, E. Bartelink, M. Finnegan, New Perspectives in Forensic Human Skeletal Identification, Chapters 19-23. Academic Press, 2018. ISBN: 978-0-12-805429-1

[4] K. Ito, A. Nikaido, T. Aoki, E. Kosuge, R. Kawamura, I. Kasima, Dental radiograph recognition system using phase-only correction for human identification. IEICE Trans. Fundamentals. 2008;E91-A(1), 298-305.

[5] E. Kosuge, K. Ito, Y. Hanzawa, T. Aoki, Large-scale performance evaluation of a dental radiograph matching system for forensic human identification. Radiological Society of North America (RSNA), 2009:1069-1070.

[6] Identification manuals, Japan Dental Association, 2012 (Oct) (in Japanese).

[7] J. Morishita, Y. Ueda, New solutions for automated image recognition and identification: challenges to radiologic technology and forensic pathology. Rad Phys and Tech, 2021;14(2), 123-133.

[8] J. Morishita, N. Ikeda, Y. Ueda, Y. Yoon, A. Tsuji, Personal identification using radiological technology and advanced digital imaging: Expectations and challenges. J of forensic Research, 2021;12(8)

[9] C O'Donnell, M Iino, K Mansharan, J Leditscke, N Woodford, Contribution of postmortem multidetector CT scanning to identification of the deceased in a mass disaster: Experience gained from the 2009 Victorian bushfires. Forensic Sci Int. 2011 Feb 25; 205(1-3): 15-18.

[10] Y. Matsunobu , J. Morishita, Y. Usumoto, M. Okumura, N. Ikeda, Bone comparison identification method based on chest computed tomography imaging. Leg Med. 2017;29:1–5.

[11] H.H. Boers, S. Blau, T. Delabarde, and L. Hackman, The role of forensic anthropology in disaster victim identification (DVI): recent developments and future prospects. 2019;4(4):303-315.

[12] LA Souza, et al, Autosomal frontal sinus recognition in computed tomography images for personal identification. Forensic Sci. Int. 2018;286:252-264.

[13] C. Virapongse, M. Sarwar, S. Bhimani, C. Sasaki, R. Shapiro, Computer tomography of temporal bone pneumatization: 1. Normal pattern and morphology. AJR, 1895;145(3):473-481.

[14] M. Isono, K. Murata, H. Azuma, M. Ishikawa, A. Ito, Computerized assessment of the mastoid air cell

system. Auris Nasus Larynx, 1999;26:139-145.
[15] Y. Kawazoe, J. Morishita, Y. Matsunobu, M. Okumura, N. Ikeda, A simple method for semi-automatic readjustment for positioning in post-mortem head computed tomography imaging. Forensic Radiol. 2019;16:57–64.
[16] J.A. Keen, A study of the differences between male and female skulls. Am J Phys Anthropol. 1950 Mar;8(1):65-79.
[17] K. Frisberg, M. Zsigmoid, The size of mastoid air cell system. Planimetry: direct volume determination. Acta Otolaryngol, 1965;20:23-29.
[18] Great East Japan Earthquake, Reconstruction Agency, https://www.reconstruction.go.jp/english/topics/GEJE/ (confirmed on Dec. 31)

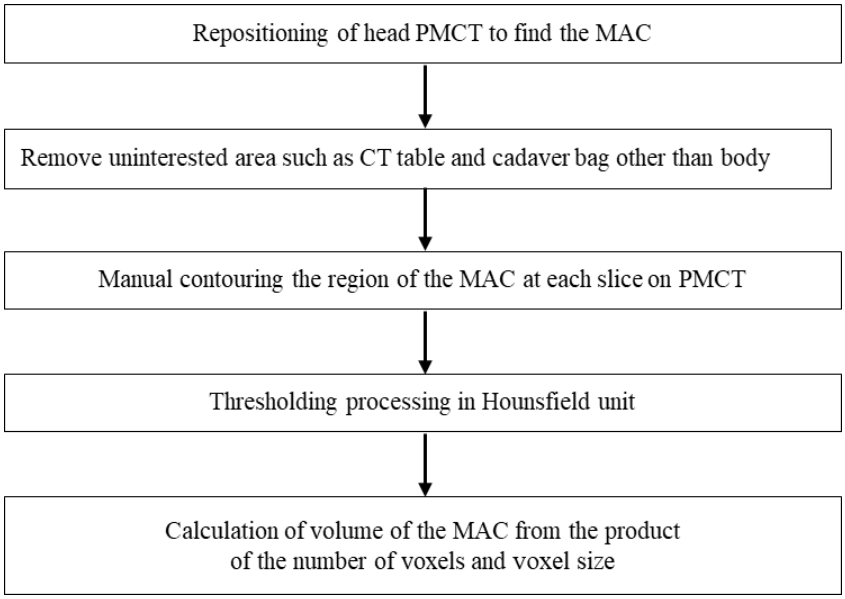

Fig. 1 Flowchart for measuring volume of the mastoid air cells (MACS) on PMCT images.

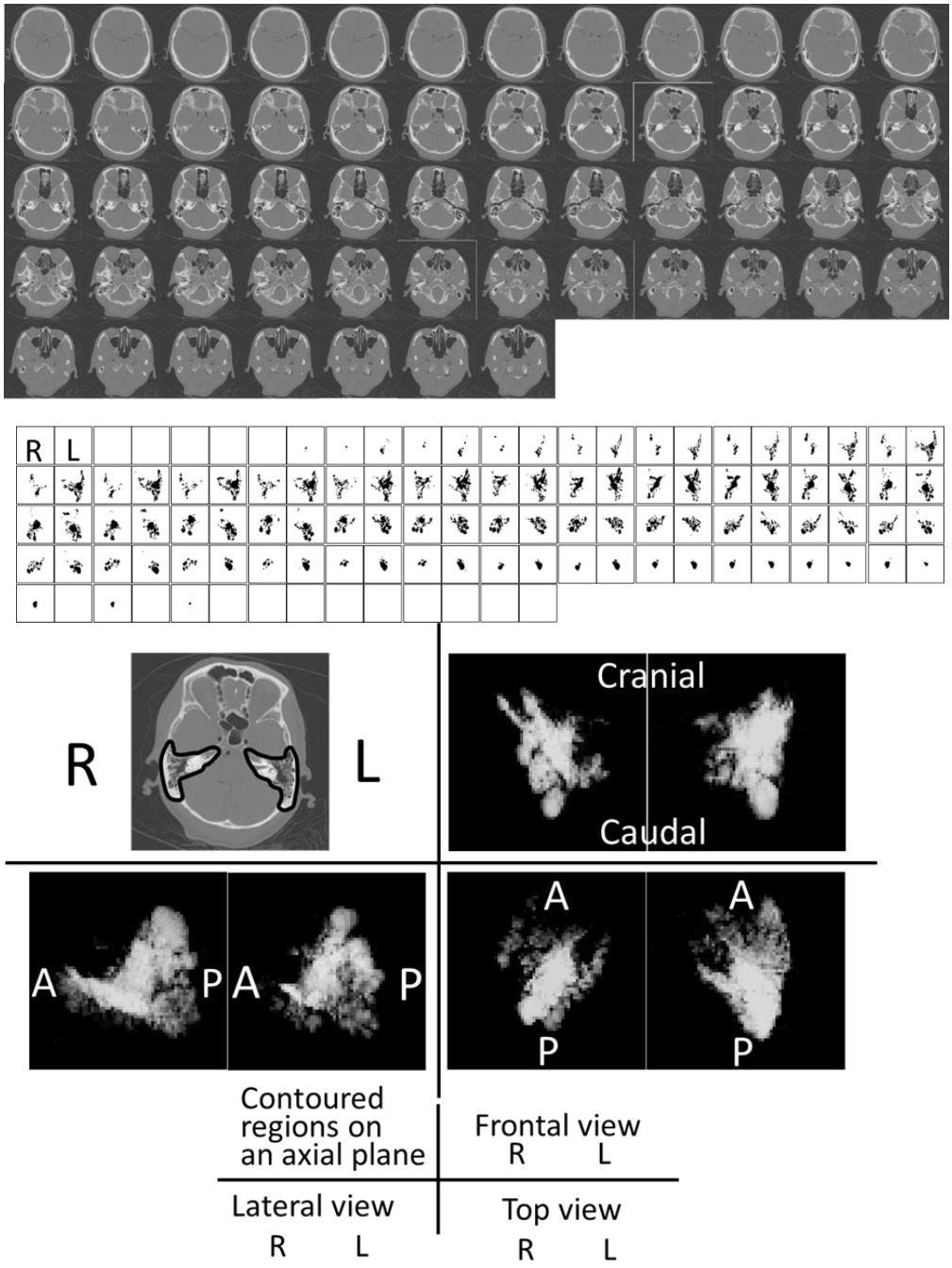

Fig. 2 An example of axial images of PMCT after repositioning (upper), binary images of both side MACs (middle), and an example of axial plane and a whole MACs in different views (bottom). White rectangle box on the top and black rectangle in the middle are the same slice. Black lines on the axial plane in the bottom indicate manually contoured regions.

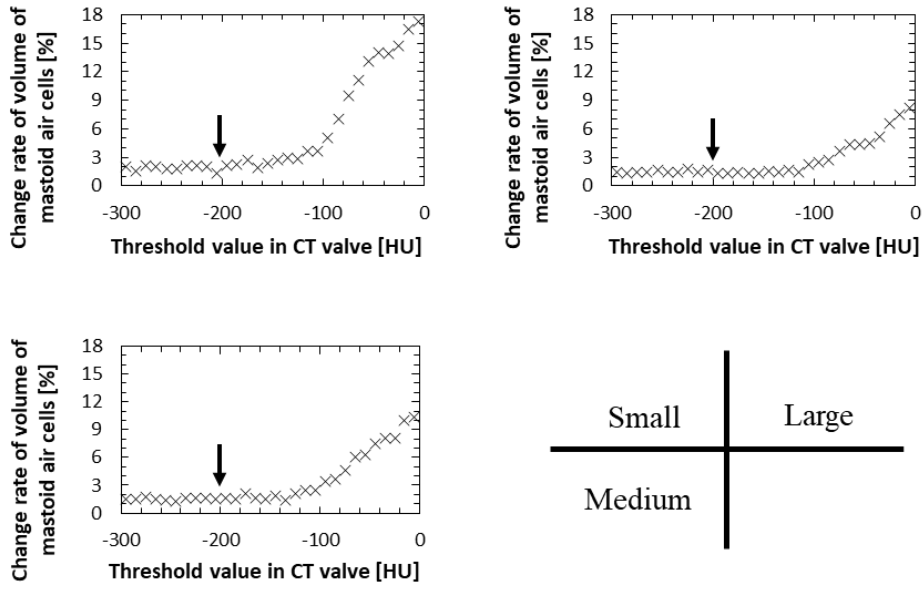

Fig. 3 Examples of the change rate of total volume of the MACs for relatively small volume (top left), medium volume (bottom left), and large-volume MACs (top right) in various threshold value. Arrows indicate threshold value at -200 HU. The threshold was chosen as a reasonable value that leads stable measurement of volume to distinguish structures bone and air cells in the temporal bone.

Table 1 Comparison of volumes and ratio of large-side MACs to small-side MACs.
＊indicates female. Numbers with underscore indicate cases where the ratio is less than 1.10.

Case number	Total Volume [mL]	Left Volume [mL]	Right Volume [mL]	Large / Small Ratio
1	0.59	0.02	0.57	28.50
2	0.93	0.41	0.52	1.25
3*	1.33	0.61	0.72	1.17
4	1.36	0.69	0.67	1.04
5	2.01	0.69	1.32	1.91
6*	2.11	1.30	0.82	1.58
7*	2.49	1.57	0.92	1.71
8	2.92	1.44	1.47	1.02
9	3.47	1.18	2.29	1.93
10*	4.10	1.89	2.21	1.17
11	4.74	2.24	2.50	1.11
12*	4.89	3.26	1.63	2.01
13	4.92	2.13	2.79	1.31
14	4.94	2.45	2.49	1.02
15	5.55	3.79	1.76	2.15
16	6.03	3.79	1.76	2.15
17*	6.12	3.93	2.19	1.79
18*	6.12	2.25	3.87	1.72
19	6.54	2.67	3.87	1.45
20	6.55	4.87	1.68	2.91
21	6.77	3.60	3.17	1.14
22	7.65	4.31	3.34	1.29
23	7.66	3.23	4.43	1.37
24*	8.13	3.74	4.39	1.18
25*	8.44	5.40	3.04	1.78
26*	8.59	4.69	3.90	1.20
27	8.97	4.07	4.89	1.20
28*	8.98	2.65	6.33	2.39
29*	9.04	4.30	4.74	1.10
30	9.09	3.15	5.94	1.89
31*	9.11	4.77	4.33	1.10
32	9.59	5.99	3.60	1.66
33*	9.74	5.24	4.50	1.17
34	10.11	6.57	3.54	1.86
35	10.37	4.82	5.55	1.15
36	10.39	4.65	5.74	1.23
37*	10.49	4.50	5.99	1.33
38	10.64	4.54	6.10	1.34
39	13.25	6.15	7.10	1.15
40	13.35	6.08	7.27	1.19
41	13.45	6.08	7.37	1.21
42	13.91	7.47	6.43	1.16
43	14.51	8.76	5.75	1.52
44	14.81	7.01	7.81	1.11
45*	14.83	7.22	7.61	1.05
46	15.41	7.91	7.50	1.06
47	15.42	8.75	6.67	1.31
48*	15.47	9.11	6.36	1.43
49	15.47	8.49	6.98	1.22
50	16.31	8.76	7.54	1.16
51	18.24	9.35	8.89	1.05
52*	18.65	10.30	8.35	1.23
53*	19.25	10.43	8.82	1.18
54*	19.69	5.87	13.82	2.35
55	19.77	11.20	8.57	1.31
56	20.15	10.51	9.63	1.09
57	23.43	12.55	10.88	1.15
58	23.59	12.94	10.65	1.22
59	24.60	13.61	10.99	1.24
60*	25.78	13.51	12.27	1.10
61	38.58	19.61	18.99	1.03
Min	0.59	0.02	0.52	1.02
Max	38.58	19.61	18.99	28.50
Average	10.97	5.62	5.34	1.85
SD	7.35	3.94	3.64	3.49

Table 2 Comparison of measured average volume in right-side and left-side MACs, and different sex.

	Average volume [mL]	Standard deviation [mL]
Right side	5.34	3.64
Left side	5.62	3.94
Male	11.40	7.79
Female	10.16	6.53

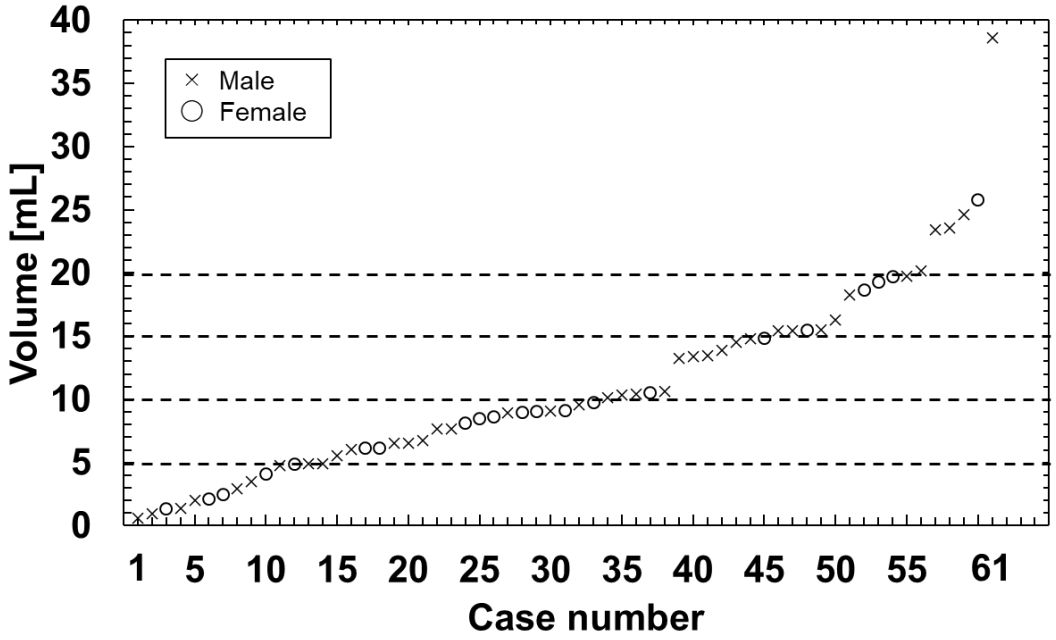

Fig. 4 shows the total volume of MACs for 61 cases. The volume varied in different persons from 0.59 to 38.58 mL, and average and standard deviation were10.97 and 7.35, respectively. Dashed lines indicate an example of rough grouping bin 5 mL interval.

Table 3 shows results obtained by grouping with 5 mL for the 61 cases.

Volume [mL]	0＜MAC≦5	5＜MAC≦10	10＜MAC≦15	15＜MAC≦20	20 <MAC
The number of cases	14	19	12	10	6

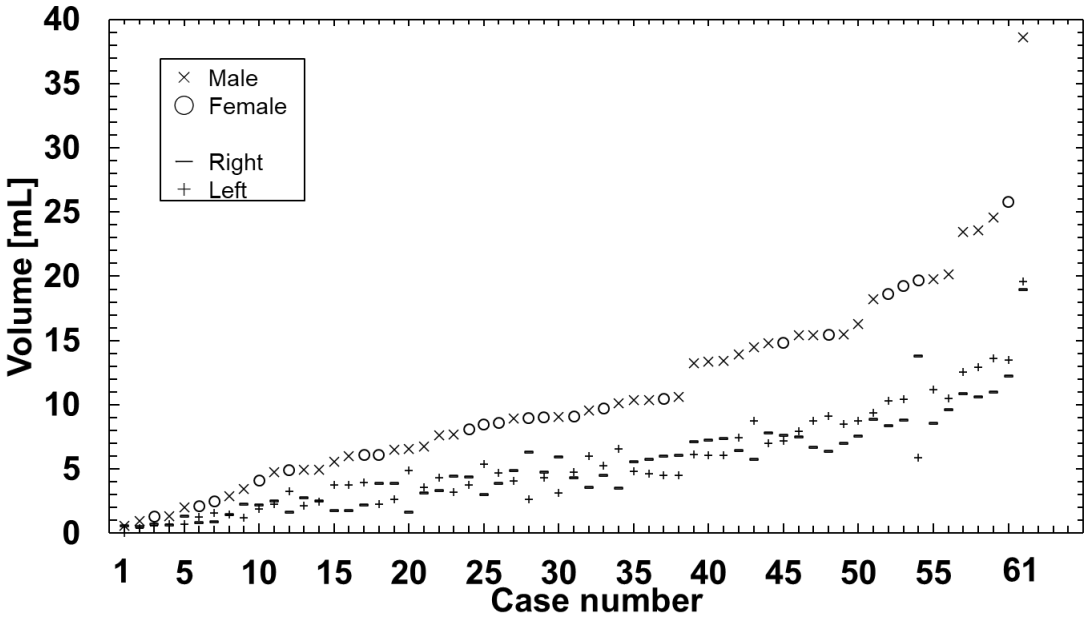

Fig. 5 Total volume (X: male O: female)) of the MACs, right-side volume (-) , and left-side volume (+) for 61 cases.

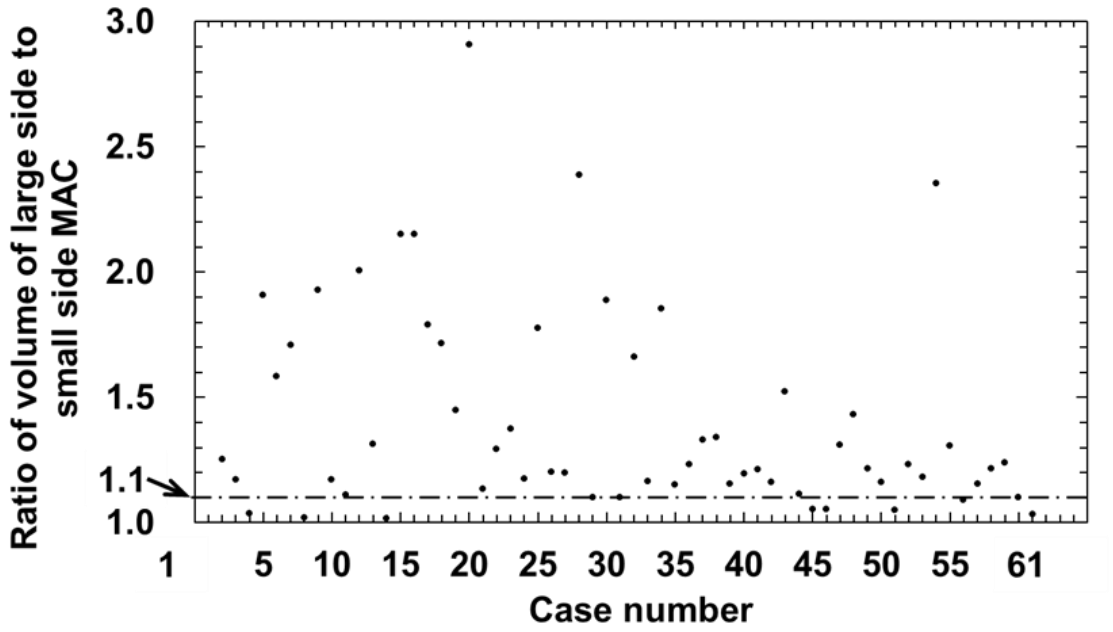

Fig. 6 Comparison of the ratio of large-side to small-side MACs. Transverse dashed line is a threshold value at a 10% difference in the ratio as an example for personal identification.